



# Drag measurements of fluttering fabrics and their application for sportswear

Franz Konstantin Fuss<sup>1,2</sup>

Accepted: 3 October 2024 / Published online: 21 November 2024  
© The Author(s) 2024

## Abstract

Loose and baggy clothing is required by the rules of ski cross and snowboard cross. However, it is known from the literature that fluttering garments increase the aerodynamic drag. The aim of this study was to investigate the influence of flexural rigidity and fabric weight on the coefficient of drag  $C_D$ . Eleven fabrics (550 mm long, 320 mm wide) with different flexural rigidity (0.016–99  $\mu\text{Nm}$ ) and fabric weight (0.1–2.4  $\text{N/m}^2$ ) were tested in a wind tunnel on a cylinder (width 325 mm, diameter 125 mm) at speeds of 25 to 120 kph (Reynolds numbers  $Re$  60 k–280 k). The general trend showed that fluttering fabrics that are heavier and stiffer create more drag force. All but one fabric had a smaller  $C_D$  than the bare cylinder in the subcritical flow regime ( $C_D \approx 1.1$ ), at least within a  $Re$  window of 80 k. One fabric had a consistently higher  $C_D$  (average: 1.27) than the bare cylinder. The mean  $C_D$  value of the other ten fabrics ranged from 0.87 to 1.07, with minimum  $C_D$  values between 0.76 and 1. The  $C_D$  advantage of the ten fabrics ended at the beginning of the critical flow regime of the bare cylinder between  $Re$  200 k and 220 k. A regression analysis showed that the magnitude of the  $C_D$  is more influenced by the flexural rigidity of a fabric, normalised to its weight, than by the weight itself, at least at  $Re < 250$  k. The results of this study suggest that ski and snowboard cross athletes' suits should be made from light and flexible fabrics to reduce aerodynamic drag.

**Keywords** Loose garments · Flexural rigidity of fabrics · Weight of fabrics · Coefficient of drag · Wind tunnel testing · Multiple regression

## 1 Introduction

In skin-tight fitting sports garments, the basic requirement is “that a fabric resist flutter in order to reduce drag force” [1]. It is well known and documented that fluttering garments increase the drag force [2]. This is why tight-fitting skin suits are preferred in sports disciplines where speed, and thus aerodynamics, are crucial, such as in alpine skiing, cycling, speed skating, swimming, or, even in sprinting. However, in some disciplines, skin suits are prohibited. In ski cross (SX) and snowboard cross (SBX), the International Ski and Snowboard Federation (FIS) has regulated the usage of clothing [3–7], which implies that there must be a gap between the

protectors (undergarment) and the competition suit (outer wear). This gap allows movements of the suit textile, usually referred to as flutter. A detailed outline of the specific clothing rules is provided in the Appendix section. Based on these rules, the question arises whether there are fabrics with defined properties that offer a competitive advantage over conventional baggy clothing (i.e., not tight-fitting skin suits). The research on fluttering textiles is very limited, probably because flutter should be avoided in the first place [1], and because fluttering garments are only required for SX and SBX.

Chua et al. [2] investigated the flutter of three loose textiles in a wind tunnel. The purpose was to analyse the effect of different looseness ratios  $\lambda$ , to evaluate how different degrees of looseness influence the coefficient of drag on a cylinder with a diameter of 220 mm. The looseness ratio  $\lambda$  was defined as the ratio of the circumferences of the textile loop (wrapped around the cylinder) to the circumference of the cylinder. A tight fit has a looseness ratio  $\lambda$  of 1. The four different  $\lambda$  tested were 1.5, 1.333, 1.167, and 1. The tight-fitting fabrics ( $\lambda = 1$ ) had a coefficient of drag ( $C_D$ ) of 1.2 in

✉ Franz Konstantin Fuss  
franzkonstantin.fuss@uni-bayreuth.de

<sup>1</sup> Chair of Biomechanics, Faculty of Engineering Science, University of Bayreuth, Bayreuth, Germany

<sup>2</sup> Division of Biomechatronics, Fraunhofer Institute for Manufacturing Engineering and Automation IPA, Bayreuth, Germany

the subcritical regime, and of 0.3–0.45 in the postcritical regime. The critical regime of the three fabrics shifted to smaller Reynolds numbers the rougher the fabric was. The  $C_D$  of the fluttering fabrics ( $\lambda > 1$ ) were consistently larger than those of the tight-fitting fabrics, with a  $C_D$  between 1.5 and 2 compared to the subcritical regime of the tight-fitting fabrics, and between 1.2 and 1.6 compared to the postcritical regime of the tight-fitting fabrics. The  $C_D$  of the fluttering fabrics showed the same trend and differed only slightly (maximally 0.2) among the three textiles. In this study, the mass per unit area was measured but the flexural rigidity of the fabrics was neglected.

Oggiano and Sætran [8] investigated the  $C_D$  of loose fabrics mounted on a cylinder and concluded that thicker fabrics have a larger  $C_D$  than thinner fabrics. They also found that smoother fabrics have a larger  $C_D$  than rougher fabrics. The thickness of fabrics is related to two fundamental properties of fabrics, namely to the area density and the flexural rigidity. Thicker fabrics made of the same material and manufacturing method are heavier and stiffer than thinner fabrics. This study implies that both the area density and the flexural rigidity affect the  $C_D$ , but it remains unclear to what extent. Oggiano and Sætran [8] drew only qualitative conclusions from their results and did not provide specific  $C_D$  data of fluttering fabrics.

In addition to fluttering fabrics mounted on cylinders, the influence of areal density and fabric stiffness on fluttering flags has also been investigated. Carruthers and Filippone [9] tested three flag fabrics with different fabric weights and stiffnesses. At aspect ratios of 10 and 20, the lightest fabric with medium stiffness had a lower  $C_D$  than the other two fabrics. The authors concluded that drag decreases with fabric weight. In contrast to this study, the experimental results of Fairthorne [10] indicate the opposite, namely that drag coefficients of fluttering flags increase with increasing area density.

According to Carruthers and Filippone [9], the fabric stiffness does not seem to have a direct influence on  $C_D$ , but does affect the smoothness of the drag curve, as stiffer fabrics are less sensitive to changes in speed. The experimental results of Martin [11] indicate that drag decreases with increasing stiffness (“*stiffer materials have reduced drag as a consequence of flexural rigidity*”), because material stiffness reduces the amplitude of flutter. In Martin’s [11] study, however, it is unclear how the material stiffness was measured or calculated (the term flexural rigidity appears only once). It could be that the dimensionless and unitless mass ratio (mass per unit area divided by the product of air density and chord length) was used as a replacement for the flexural rigidity (the shorter and heavier, the stiffer). However, when testing flags of equal chord length at the same air density, then mass ratio and the mass per unit area of the materials must be proportional. This is clearly not the case when using

the data provided on page 103 of Martin [11] (where the unit of the mass per area is given in kg).

The drag behaviour of fluttering flags does not necessarily hold true for fluttering fabrics mounted on a cylinder, since the looseness ratio  $\lambda$  becomes extremely large in flags. Nevertheless, not only in flags, but also in loose and fluttering textiles mounted on a cylinder, the influence of area density and the flexural rigidity on the coefficient of drag is still unclear. Therefore, the aim of this study is to investigate (1) how the area density and the flexural rigidity influence the aerodynamic drag of loose fabrics; (2) whether the  $C_D$  of loose fabrics can be smaller than the  $C_D$  of a bare cylinder, particularly in the subcritical regime; and (3) which fabric property has a greater influence on the  $C_D$  at which Reynolds number ( $Re$ ).

## 2 Material and methods

### 2.1 Fabrics

#### 2.1.1 Selection of fabrics

From the fundamentals of multiple regression, if two predictors (independent variables) correlate too well with each other, then their shared (combined) influence on the response variable (dependent variable) is very large, whereas their unique (individual) influence on the response variable is negligible. It was therefore paramount to select a variety of fabrics, the properties of which (flexural rigidity and area density) do not correlate well in the first place. It is expected that there is some correlation between flexural rigidity and area density, namely the heavier, the stiffer (the mathematical explanation for this relationship will be provided later in this document), and that extreme and opposite conditions cannot be found easily (light and stiff; heavy and soft). The selection process was therefore empirical rather than systematic. The starting point was the three fabrics used in an earlier study [2]. Further fabrics were mostly obtained from retail, i.e., from second-hand shops to specialised textile stores. The details of the fabrics are shown in Table 1. The eleven fabrics are illustrated in Fig. 1.

#### 2.1.2 Fabric properties

The areal density of the fabrics, also known as GSM (grams per square metre) or fabric ‘weight’, was measured according to the ASTM D3776 [12]. The areal density is subsequently denoted  $\rho_F$ , expressed in  $\text{g/m}^2$ ; and the weight of the fabric is denoted  $w$ , expressed in  $\text{N/m}^2$ ,

$$w = \frac{\rho_F}{1000} g \quad (1)$$

**Table 1** Fabric details and properties

ID	Description	$w$ (N/m <sup>2</sup> )	$G_{GT}$ (μNm)	$G_P$ (μNm)	$G_{nGT}$ (cm <sup>3</sup> )	$G_{nP}$ (cm <sup>3</sup> )
<i>Knitted fabrics</i>						
J	Reverse stockinette interlock based mock mesh double jersey	2.305	3.424	2.917	1.485	1.265
W	Reverse stockinette interlock based mock mesh double jersey	1.864	1.081	1.034	0.580	0.555
P	Warp-knit fabric charmeuse	1.584	0.429	0.583	0.271	0.368
O	Sportwool™, reverse stockinette composite fabric (2 layers)	2.139	2.102	2.803	0.983	1.311
B	Warp-knit fabric charmeuse	2.439	8.172	9.232	3.351	3.785
<i>Woven fabrics</i>						
Y	Coated fabric	1.432	98.99	84.59	69.12	59.06
I	Cambric	0.503	2.645	2.430	5.256	4.828
D	Crepe lavable	0.361	0.580	0.581	1.608	1.608
G	Silk georgette	0.336	0.681	0.602	2.025	1.789
C	Silk chiffon	0.256	0.527	0.502	2.057	1.960
T	Silk tulle	0.114	0.016	0.019	0.140	0.163

ID identification code used throughout this document (fabric J was the official jersey of the Australian team in ski- and boarder-cross at the 2010 Vancouver Olympic Games);  $w$ : fabric weight;  $G_{GT}$ : flexural rigidity measured with the method of Grießer and Taylor [14];  $G_P$ : flexural rigidity measured with Peirce’s [17] method;  $G_{nGT}$ :  $G_{GT}$  normalised to  $w$ ;  $G_{nP}$ :  $G_P$  normalised to  $w$

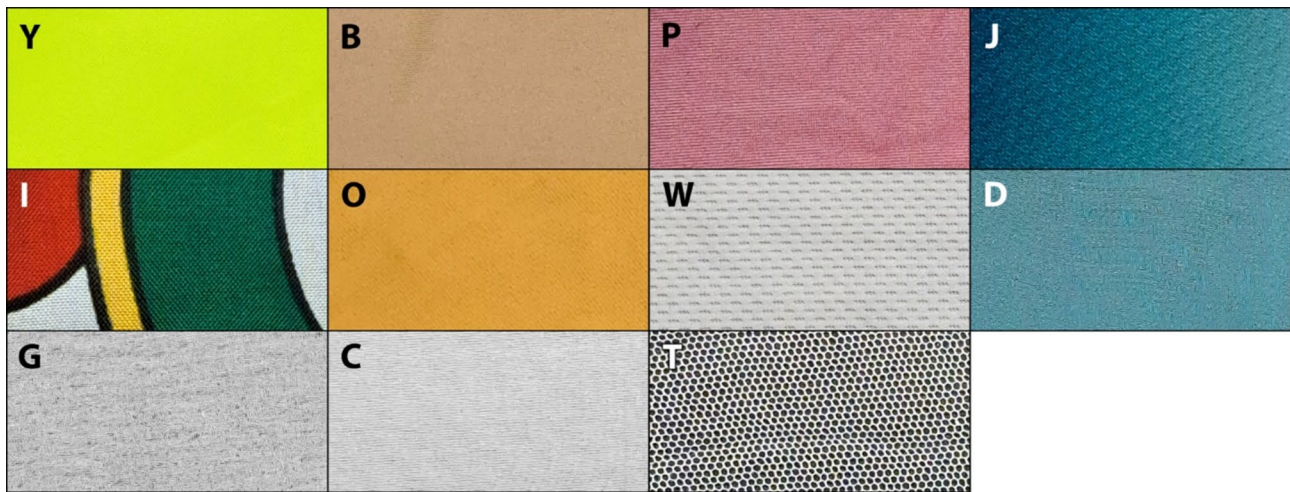


**Fig. 1** Images of the fabrics analysed in this study; the identification code in the top left corner of each fabric sample is the same as in Table 1; the size of the sub-figures corresponds to fabric samples of 50 mm by 25 mm

where  $g$  denotes the gravitational acceleration (in m/s<sup>2</sup>).

The flexural rigidity of the fabrics was measured from two methods: a modified ASTM D1388 [13], and a modified Grießer-Taylor method [14].

The Cantilever Test of the ASTM D1388 standard [13] employs the principle of cantilever bending of the fabric under its own weight (Fig. 2a) This test is usually carried out with a Shirley tester of a slope angle  $\theta$  of 41.5°. Three samples (weft direction: 152 mm, warp direction: 25 mm) of each fabric were tested four times in opposite

directions. The modification of the test was that the slope angle  $\theta$  of the Shirley tester was set to 42.9° [15], although the error in measurement would be small [16] when using the original 41.5°. According to Peirce [17]

$$C = L f_{\theta} \tag{2}$$

where  $C$  is the bending length of the fabric strip (Fig. 2a),  $L$  is the length of the fabric projecting (i.e. the length of the overhanging fabric strip), and  $f_{\theta}$ , a function of the inclination angle  $\theta$ , is

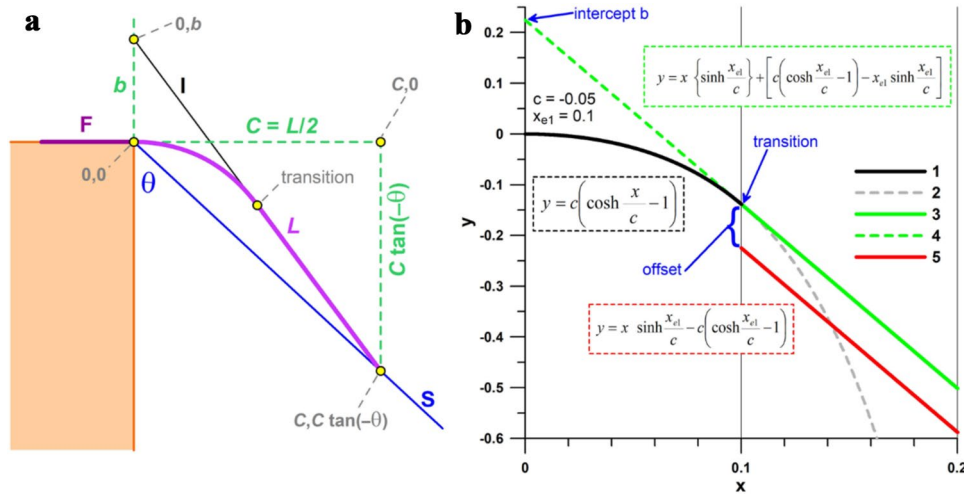


**Fig. 2** Method for determining the flexural rigidity of a fabric; **a** principle of the Shirley tester; F: part of fabric on the horizontal part of the Shirley tester; “0,0”: origin of the coordinate system (edge of the horizontal part); L: length of the overhanging part of the fabric; I: extrapolation of the straight part of the fabric; b: intercept of I; C=bending length; S=slope of the Shirley tester;  $\theta$ =slope angle (42.9°); transition: between bent and straight parts of the fabric; **b**

$c$  &  $x_{e1}$ : coefficients of the hyperbolic functions; 1: bent part of the fabric (from edge to transition); 2: hypothetical continuation of the bent part; 3: straight part of the fabric (after the transition); 4: hypothetical continuation of the straight part; 5: straight part according to the original equation of Grießer and Taylor [14]; offset: discontinuity between bent and straight parts when using Grießer and Taylor’s equation

$$f_{\theta} = \sqrt[3]{\frac{\cos \frac{\theta}{2}}{8 \tan \theta}} \quad (3)$$

If  $f_{\theta}$  is set to 0.5, the corresponding inclination angle is 42.94°, and  $C=L/2$  (unit: m). The flexural rigidity  $G_p$  (unit: Nm, preferably expressed in  $\mu\text{Nm}$ ) is then calculated from

$$G_p = w C^3 \quad (4)$$

Equation (4) explains the aforementioned mathematical relationship between  $\rho_F$  (or  $w$ ) and  $G_p$ : the heavier, the stiffer the fabric.

The Grießer-Taylor method [14] was not only used for comparison purposes but rather for two specific reasons.

- (1) The cantilever test (Peirce’s method [17]) hinges on the pure bending theory of an elastic beam bending within the limit of linear strain, which implies a linear relationship between the curvature of the bent fabric and the bending moment. The large deflections, especially in soft fabrics, could exceed the linear regime. The new approach of Grießer and Taylor [14] overcomes this problem and uses potential and bending energy as parameters.
- (2) Fabrics require a threshold moment to initiate bending [18]. Therefore, the overhanging part of the fabric sample in the Shirley tester is not continuously bent but has a curved and a straight part (Fig. 2). This property

was implemented in the Grießer-Taylor method [14] which allows to calculate the bending stiffness from experimental data and the bending shape as an analytical function.

The Grießer-Taylor method [14] was modified because two of their equations were incomplete. This method hinges on the principle that a fabric strip, when slid over an edge (comparable to the Shirley method) has a bent and a straight part (Fig. 2b). Fitting a straight line to the straight part delivers two points, the intercept  $b$  of the straight line with the  $y$ -axis ( $x_1=0, y_1=b$ ), and the endpoint of the overhanging fabric ( $x_2, y_2$ ). The origin of the coordinate system is right at the edge. The slope of the straight line,  $(y_2-y_1) / (x_2-x_1)$ , is denoted  $m$ . Slope  $m$  and intercept  $b$  are related to a curvature parameter  $c$  and to the  $x$ -coordinate ( $x_{e1}$ ) of the point separating bent and straight parts. According to Eq. 13 of Grießer and Taylor [14], the bent and straight parts of the fabric are modelled as follows:

$$y = c \left( \cosh \frac{x}{c} - 1 \right) \quad \text{if } 0 < x < x_{e1} \quad (5)$$

$$y = mx + b \quad \text{if } x_{e1} < x \quad (6)$$

where

$$m = \sinh \frac{x_{e1}}{c} \quad (7)$$

$$b = -c \left( \cosh \frac{x_{e1}}{c} - 1 \right) \quad (8)$$

However, as Eq. (8) leads to a discontinuity at the transition from the bent to the straight part (Fig. 2b), the equation of Griebner and Taylor [14], i.e., Eq. (8) above, was modified to

$$b = +c \left( \cosh \frac{x_{e1}}{c} - 1 \right) - x_{e1} \sinh \frac{x_{e1}}{c} \quad (9)$$

The correctness of Eq. (9) was confirmed by Taylor (personal communication, 2013) and by Griebner (personal communication, 2013).

From  $m$  and  $b$ ,  $c$  and  $x_{e1}$  were calculated from Eqs. (7) and (9) by substitution:

$$c = \frac{b}{\cosh(\sinh^{-1} m) - 1 - m \sinh^{-1} m} \quad (10)$$

$$x_{e1} = c \sinh^{-1} m \quad (11)$$

The flexural rigidity  $G_{GT}$  (unit: Nm, preferably expressed in  $\mu\text{Nm}$ ) of the fabric results from modifying Eq. 15 of Griebner and Taylor [14]:

$$G_{GT} = \frac{k_1 + k_2 + \frac{k_3}{w}}{k_4} w \quad (12)$$

As  $k_3$  did not have the same unit as  $k_1$  and  $k_2$ , the original Eq. 15 of Griebner and Taylor [14] had to be modified by dividing  $k_3$  by  $w$ . This modification was provided by Taylor (personal communication, 2013). The terms of Eq. (12),  $k_1$ ,  $k_2$ ,  $k_3$ , and  $k_4$  are detailed in Griebner and Taylor [14].

Both flexural rigidities,  $G_P$  and  $G_{GT}$ , were simultaneously determined from each test from Eqs. (4) and (12) with the modified Shirley tester. As the weight  $w$  of the fabrics is required for calculating the flexural rigidities, the latter were normalised to  $w$  to avoid any confounding factors when correlating these two properties.

Since the fabric properties  $w$ ,  $G_P$  and  $G_{GT}$  were widely scattered (minimum and maximum data differed by more than one, and almost four orders of magnitude, respectively; Table 1), the property data were logarithmically transformed. The agreement of the  $\log G_P$  and  $\log G_{GT}$  (as well as  $\log G_{nP}$  and  $\log G_{nGT}$ ) data was assessed by linear correlation (proximity of the slope to unity and the intercept to zero) and compared for any significant differences using a nonparametric test for correlated samples (Wilcoxon signed rank test). This agreement is important because Peirce's method [17] is limited to a linear relationship between the curvature of the bent tissue and the bending moment.

## 2.2 Wind tunnel testing

The fabrics were tested with the same method as used by Fuss [19] and Chua et al. [2] in the RMIT Industrial Wind Tunnel (closed return circuit, maximum speed 150 km/h, turbulence intensity of 1.8% [20]). The fabrics were mounted on a test rig, consisting of a steel cylinder (Fig. 3a) of 325 mm width and 125 mm diameter with circular splitter plates (diameter 660 mm) attached to each side. The test rig was mounted on a force plate (Type 9260AA6, Kistler, Winterthur, Switzerland) in the wind tunnel. The fabric samples were 550 mm long (weft direction) and 320 mm wide (warp direction), resulting in a looseness ratio of  $\lambda = 1.4$ . The samples were wrapped around the cylinder with their free ends taped to the cylinder at the front stagnation line. The fabrics

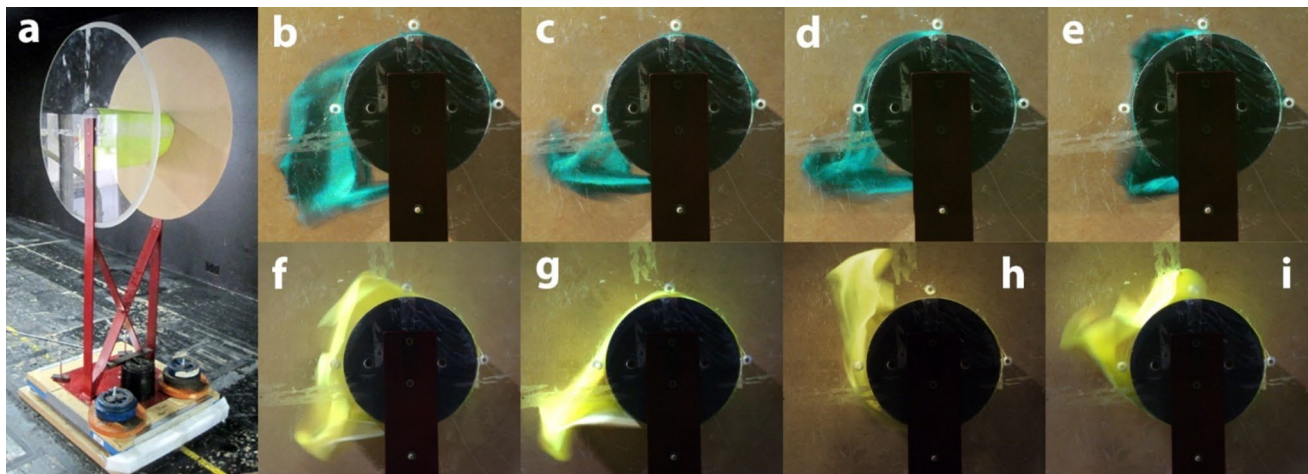


**Fig. 3** a Test rig with splitter plates and fabric Y wrapped around the cylinder; b-e fabric D fluttering at  $Re = 150 \text{ k}$ ; f-i fabric Y fluttering at  $Re = 150 \text{ k}$

and the bare cylinder were each tested three times by continuously increasing the free airflow velocity  $v$ , provided by the pitot-static tube mounted in the tunnel, up to a maximum  $v$  of 35 m/s (126 kph,  $Re = 296$  k). The horizontal drag force  $F_D$  acting on the test rig and  $v$  were recorded concurrently at a frequency of 100 Hz.

The dimensions of the cylinder (diameter) and the fabrics (weft length) were based on the FIS clothing regulations. Rule 6 of the SX rules [5] specifies that when the ski suit is pulled forward on the thigh and upper arm, the distance between the front edge of the fabric and the skin of the thigh and upper arm must be 80 and 60 mm respectively. The measuring tool mentioned in the rules [4, 5] is available from Settele Ltd. (Lindenberg, Germany) [6]. Therefore, a cylinder diameter was chosen that fits between a normal muscular thigh and upper arm, and a looseness ratio that produces the above-mentioned distance between 60 and 80 mm.

For data processing, the horizontal force data were tared, by subtracting the test rig's drag force (without cylinder) from the experimental data (cylinder without and with fabric samples). The blockage ratio of 1.17% was considered negligible and therefore not corrected. The force-speed data of all three tests per fabric were combined, sorted for speed, and filtered with a rolling average of 25 data. The coefficient of drag  $C_D$  was calculated from

$$C_D = \frac{2 F_D}{\rho_a A v^2} \quad (13)$$

where  $A$  is the frontal area of the cylinder and  $\rho_a$  is the density of air.

The measurement uncertainty was calculated for each fabric across a window of  $60 \text{ k} \leq Re \leq 280 \text{ k}$  from averaging the  $C_D$  data of the three tests per fabric at similar  $Re$ , subtracting the mean from the original  $C_D$  data, and calculating the standard deviation of the differences (about 5000 data per fabric).

### 2.3 Statistical calculations

As the weight  $w$  of the fabrics is required for calculating their flexural rigidities, the latter were normalised to  $w$  to avoid any confounding factors when correlating  $w$  and  $G_{nP}$  or  $G_{nGT}$  (unit:  $\text{cm}^3$ , as  $\text{centi}^3 = \text{micro}$ ) with the drag coefficient  $C_D$ :

$$G_{nP} = \frac{G_P}{w} = C^3 \quad (14)$$

$$G_{nGT} = \frac{G_{GT}}{w} = \frac{k_1 + k_2 + \frac{k_3}{w}}{k_4} \quad (15)$$

As a power function provided a good fit when correlating  $w$  and  $G_{nP}$  or  $G_{nGT}$ , these properties in their logarithmic form were ultimately correlated to the mean  $C_D$  of each fabric at different  $Re$  (60 k to 280 k in steps of 10 k), to identify the unique (individual; squared semi-partial correlation coefficients  $R_A^2$ ,  $R_C^2$ ) and shared (combined;  $R_B^2$ ) influence of two predictors (independent variables  $w$  and  $G_{nP}$  or  $G_{nGT}$ ) on the response variable (dependent variable  $C_D$ ). A multiple regression ( $R_{ABC}^2$ ) was rejected based on at least one of the following criteria: (1) at least one of the two squared partial correlation coefficients ( $R_{AB}^2$  or  $R_{BC}^2$ ) was insignificant ( $R^2$  p-value  $> 0.1$ ;  $\alpha = 0.1$  in regression  $R^2$ ); (2) the shared component ( $R_B^2$ ) was negative; and (3) the variance inflation factor ( $VIF = (1 - R_{ABC}^2)^{-1}$ ) was greater than five [21].  $R_A^2$ ,  $R_B^2$ , and  $R_C^2$  were calculated from:

$$R_B^2 = R_{AB}^2 + R_{BC}^2 - R_{ABC}^2 \quad (16)$$

$$R_A^2 = R_{AB}^2 - R_B^2 \quad (17)$$

$$R_C^2 = R_{BC}^2 - R_B^2 \quad (18)$$

## 3 Results

### 3.1 Fabric behaviour and properties

Figure 3b–i shows examples of the behaviour of the fabrics when mounted on the cylinder in the wind tunnel. The more flexible fabric D (Fig. 3b–e) flutters with a lower amplitude than the stiffer fabric Y (Fig. 3f–i). The fabrics usually follow the curvature of the front half of the cylinder, while the fabrics on the back half detach from the contour and billow and flutter. The separation can be completely on the back half (Fig. 3b) or more pronounced on the upper and lower halves with slight detachment in the centre back (Fig. 3f) or no detachment in the centre back (Fig. 3e). The fabrics can form a tail in the lower back quarter (Fig. 3c,g) or in the upper back quarter (Fig. 3h) that represents the typical flutter when occurring in rapid succession; or in the lower back quarter with billowing in the upper back quarter (Fig. 3d). Figure 3i shows a short tail in the centre of the back half and a billow in the upper back quarter.

The flexural rigidities obtained from the methods of Peirce [17] and Grießer and Taylor [14], before ( $G_P$  and  $G_{GT}$ ) and after normalisation ( $G_{nP}$  and  $G_{nGT}$ ) to the fabric weight  $w$ , correlated well with  $R^2 = 0.9944$  ( $\log G_P = 0.9696 \log G_{GT} + 0.0136$ ) and  $R^2 = 0.9922$  ( $\log G_{nP} = 0.9381 \log G_{nGT} + 0.0234$ ). When compared with a non-parametric test for correlated samples (Wilcoxon Signed-Rank Test),  $\log G_P$  and  $\log G_{GT}$  (as well as  $\log G_{nP}$  and  $\log G_{nGT}$ ) are not

significantly different ( $p=0.9442$ ), which confirms that the results of both flexural rigidity tests are the same.

Table 1 shows the values of the fabric properties  $w$  and  $G$ . The margin of error ( $MoE_{0.95}$ ) for  $w$  ranged between 1.18% and 2.20% of the mean values. The heavier the fabric, the higher the  $MoE_{0.95}$ . The  $MoE_{0.95}$  for  $G_p$  and  $G_{GT}$  ranged between 1.39% and 5.36%, and between 1.97% and 9.77%, respectively. The stiffer the fabric, the smaller the  $MoE_{0.95}$ . The  $MoE_{0.95}$  of  $G_{GT}$  was higher than that of  $G_p$ , because the calculation of  $G_{GT}$  requires two input parameters ( $L$  and  $b$ ; Fig. 1) while that of  $G_p$  requires only one ( $L$ ).

Figure 4a shows the correlations between  $\log G$  and  $\log w$ , with  $R^2$  of 0.4571 ( $G_{GT}$ ) and 0.4983 ( $G_p$ ). When normalising  $G$  to  $w$  (Fig. 4b), these correlations are not significant, with  $R^2$  of 0.0545 ( $p=0.4891$ ;  $G_{nGT}$ ) and 0.0687 ( $p=0.4375$ ;  $G_{nP}$ ), which indicates that the two variables,  $G_n$  and  $w$ , are independent. However, there are two distinct clusters (Fig. 4c), cluster 1 comprising of *knitted* fabrics J, W, P, O, B (Table 1) with larger  $w$ , and cluster 2 comprising of *woven* fabrics Y, I, D, G, C, T with smaller  $w$ . The density  $w$  of each cluster correlates highly with  $G_n$  (Fig. 4c). Due to the two different manufacturing methods of two fabrics that share the same flexural rigidity, the *woven* fabric is significantly lighter than the *knitted* fabric.

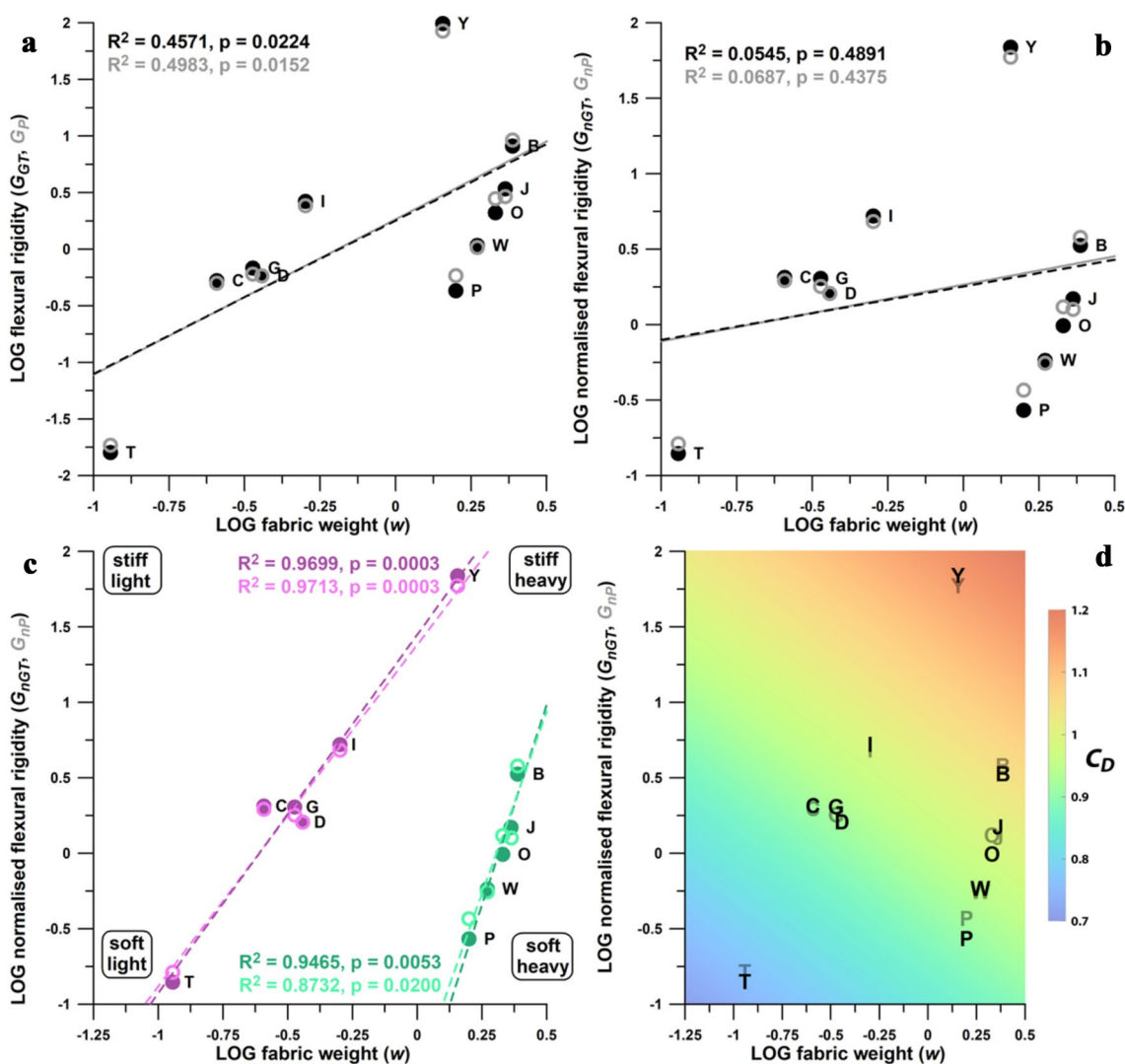


**Fig. 4** Logarithm of flexural rigidity  $G$  versus logarithm of the fabric weight  $w$ ; filled circle:  $G_{GT}$  or  $G_{nGT}$  ( $G$  measured with the Griebner-Taylor method [14]; subscript  $n$  indicates the normalised  $G$ );  $\circ$ :  $G_p$  or  $G_{nP}$  ( $G$  measured with Peirce’s method [17]; subscript  $n$  indicates the normalised  $G$ ); **a**  $\log G$  vs  $\log w$ ; **b**  $\log G_n$  vs  $\log w$ ; **c**  $\log G_n$  vs

$\log w$ , correlation of the individual clusters; purple: woven fabrics; green: knitted fabrics; **d**  $\log G_n$  vs  $\log w$ , and the expected corresponding colour-coded  $C_D$  from Eq. (19); the identification code of the fabrics is the same as in Table 1

### 3.2 Drag measurements

Figure 5 shows the  $C_D$  of the fluttering fabrics and the  $C_D$  of the bare cylinder (subcritical and critical flow regimes) at  $60 \text{ k} \leq Re \leq 280 \text{ k}$ . We can distinguish four different groups based on the mean  $C_D$ . Group 1 and 2 consist only of one fabric each, characterised as follows: the  $C_D$  of group 1, fabric Y, is consistently larger than that of the bare cylinder; the  $C_D$  of group 2, fabric B, is smaller than that of the bare cylinder only within a small  $Re$ -window, at  $110 \text{ k} \leq Re \leq 190 \text{ k}$ . Group 3 comprises of fabrics P, J, I, O, and W, all of which have a consistently smaller  $C_D$  than fabric B at  $Re > 65 \text{ k}$ , and smaller than the bare cylinder at  $80 \text{ k} \leq Re \leq 200 \text{ k}$ . Group 4 comprises of the fabrics D, G, C, and T, all of which have a consistently smaller  $C_D$  than group 3 at  $Re > 65 \text{ k}$ , and smaller than the bare cylinder at  $70 \text{ k} \leq Re \leq 210 \text{ k}$ . Fabrics C and T, with the lowest mean  $C_D$  have minimum  $C_D$ -values at  $Re \approx 115 \text{ k}$ , namely  $C_D = 0.8535$  and  $C_D = 0.7650$ , respectively. The uncertainty of the drag measurements ranged between  $\pm 0.0107$  and  $\pm 0.0210$  (in terms of  $C_D$ ), the larger  $\log w$ , the larger was the uncertainty, and also the fluctuations of the mean  $C_D$ .

### 3.3 Correlation analysis

The general trend emerging from the correlation analysis is that the stiffer (larger  $G_n$ ) and the heavier (larger  $w$ ) the fabric, the larger the  $C_D$ .

Figure 6 shows the multiple regression analysis and the corresponding tree-way Venn diagram (Fig. 6a). A multiple regression analysis is neither applicable at  $Re < 90 \text{ k}$ , since the p-value of  $R_{AB}^2$  is greater than 0.1 (Fig. 6b) nor at  $100 \text{ k} \leq Re \leq 140 \text{ k}$ , since VIF is greater than 5 (Fig. 6c).

**Fig. 5** Coefficient of drag  $C_D$  versus Reynolds number and free-stream velocity measured in the wind tunnel;  $K$  = bare cylinder; the colour-coded fabrics Y–T are detailed in Table 1; the colour-coding of the fabrics as well as their average  $C_D$  across  $60 \text{ k} \leq Re \leq 280 \text{ k}$  is shown in the rectangular inset

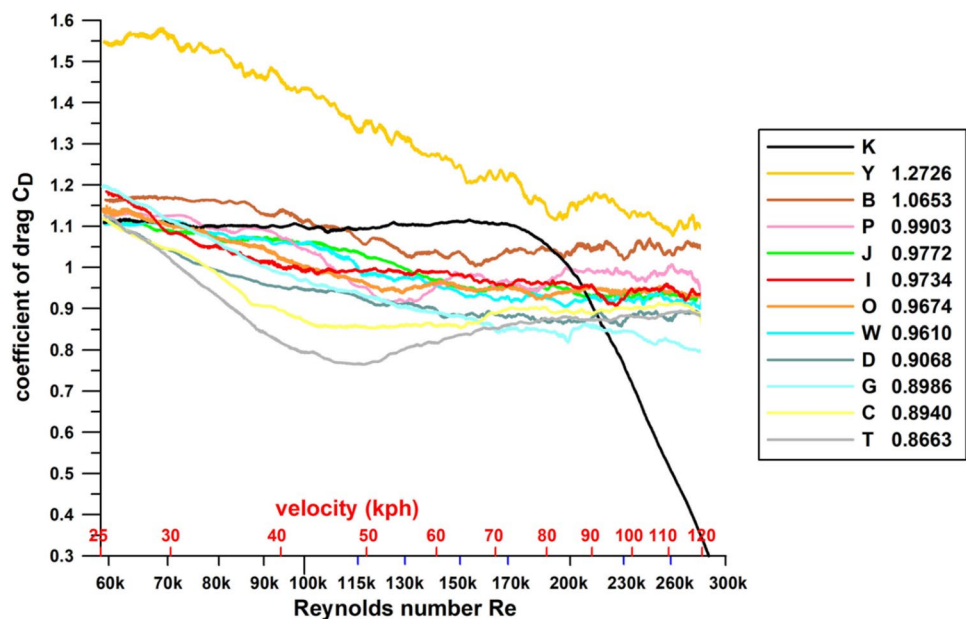


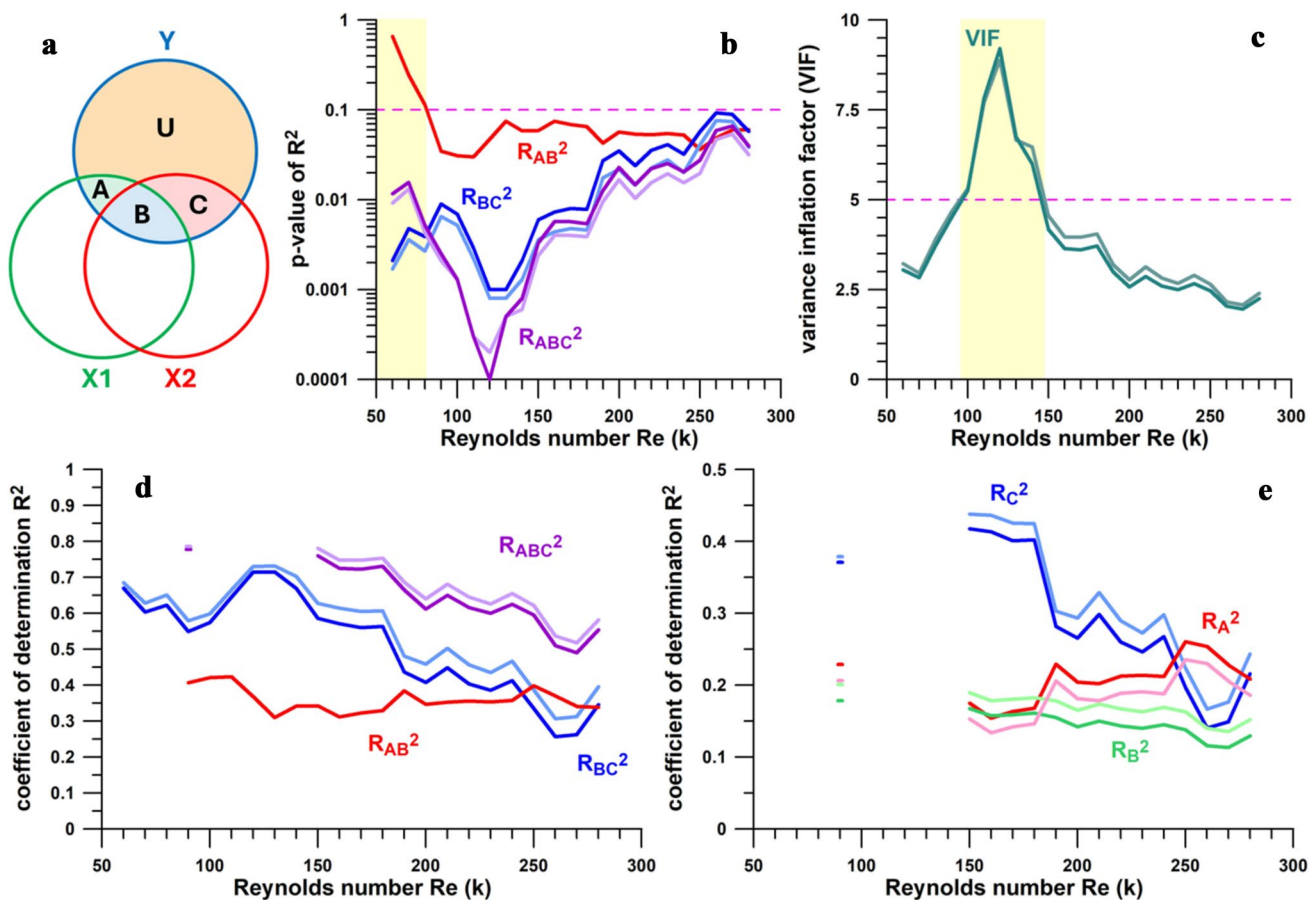
Figure 6d shows the multiple regression  $R_{ABC}^2$ , and partial  $R_{AB}^2$  and  $R_{BC}^2$ . The influence of the normalised flexural rigidity ( $G_{nGT}$ ,  $G_{nP}$ ) on the  $C_D$  is greater than that of the fabric weight  $w$ . At  $Re = 130 \text{ k}$ , 70% of  $C_D$  is explained from  $G_n$ , and 30% from  $w$ . At  $150 \text{ k} \leq Re \leq 170 \text{ k}$ ,  $R_C^2$ , the unique influence of  $G_n$  on  $C_D$ , is around 42%;  $R_A^2$ , the unique influence of  $w$  on  $C_D$  is 15%; and  $R_B^2$ , the shared influence, is 17% (Fig. 6e). As  $Re$  increases,  $R_C^2$  decreases,  $R_A^2$  increases slightly, and  $R_B^2$  decreases marginally. At  $Re \leq 200 \text{ k}$ , i.e., before the end of the subcritical regime,  $G_n$  has a substantially greater influence on  $C_D$  than  $w$ .

Figure 4d shows the expected  $C_D$  at  $Re = 150$ , calculated from the multiple regression equation:

$$C_D = 0.9451 + 0.1037 \log(w) + 0.1056 \log(G_n) \quad (19)$$

## 4 Discussion

This study shows that fluttering garments are not necessarily disadvantageous. Ten out of eleven fabrics with varying  $G$  and  $w$  had a smaller  $C_D$  than the bare cylinder, at least across a Reynolds number window of 80 k width. The magnitude of the  $C_D$  seems to depend on two opposing mechanisms, a splitter-plate-equivalent effect, and billowing of the fabric. One mechanism is the drag reduction with rigid splitter plates and fairings attached to the back of a cylinder [22]. However, loose fabrics are not rigid but flutter. In oscillating splitter plates,  $C_D$  depends on the amplitude and frequency  $f$  of the oscillations [23]. As a rule of the thumb, at low non-dimensional frequencies ( $f_s < 0.18$ ;  $f_s = f \times \text{free-stream velocity} / \text{diameter of cylinder}$ ), the larger the amplitude,



**Fig. 6** Multiple regression analysis; **a** Venn diagram; X1, X2: predictors (log weight & log normalised flexural rigidity, respectively); Y: response variable (coefficient of drag); U: component of Y not explained from X1 and X2; A: component of Y uniquely explained by X1 ( $R_A^2$ ); C: component of Y uniquely explained by X2 ( $R_C^2$ ); B: component of Y commonly explained by X1 and X2 ( $R_B^2$ ); the area shaded in yellow indicates that a multiple regression is not justified in this Reynolds number range; **b** p-value of  $R_{AB}^2$  ( $R_A^2 + R_B^2$ ),  $R_{BC}^2$  ( $R_B^2 + R_C^2$ ), and  $R_{ABC}^2$  ( $R_A^2 + R_B^2 + R_C^2$ ) versus the Reynolds number

$Re$ ; the dashed line indicates the significance threshold ( $\alpha=0.1$ ); **c** variance inflation factor VIF versus  $Re$ ; the dashed line indicates the VIF threshold (5); **d** multiple regression  $R_{ABC}^2$  and squared partial correlations  $R_{AB}^2$  and  $R_{CB}^2$  versus  $Re$ ; **e** squared semi-partial correlations  $R_A^2$  and  $R_C^2$  and the squared shared correlation  $R_B^2$  versus  $Re$ ; **b-e** lighter colours refer to  $\log G_{np}$  (normalised flexural rigidity calculated with Peirce’s method [17]); darker colours refer to  $\log G_{nGT}$  (normalised flexural rigidity calculated from the Grießer-Taylor method [14])

the greater is the  $C_D$  [23]. Heavier and stiffer fabrics flutter with larger amplitude behind the cylinder. The other mechanism is the detachment of the fabric from the surface of the cylinder. Unstable and rapidly changing low pressure zones due to increased turbulence cause billowing of the fabric on the cylinder which increases the wake by moving the flow separation line closer to the front stagnation point. Therefore, the drag force increases. Billowing is apparent in Fig. 3d,e,f,i. The two opposing mechanisms are controlled by  $w$  and  $G_n$  of the fabric. Softer and lighter fabrics adapt to the air stream with less frequent billowing and more splitter-plate-equivalent effect (smaller flutter amplitude). The stiffest fabric Y fluttered violently with rapid movements, causing a loud noise in the wind tunnel. Since the product of  $w$  and  $G_n$  equals  $G$ , the flexural rigidity  $G$  can be regarded as the decisive fabric property that influences the  $C_D$ .

Further parameters would be the air permeability and the roughness of a fabric [1] which are probably more applicable to skin-tight fitting sports garments. It is doubtful that air can flow effectively through the pores of a fabric when it flutters at a high frequency at large translational and angular velocities, such that sections of the fabric change their angular orientations constantly. As for roughness, the height of the roughness elements of a fabric is several orders of magnitude smaller than the flutter amplitude (Fig. 3gh). Therefore, roughness cannot have any significant impact on drag in fluttering fabrics (but it can in tight fitting skin suits). Fabric wetness seems to have an influence on the fabric aerodynamics as well, as dry fabrics provide “slightly less drag” than wet fabrics [1] except for coated fabrics. In fluttering fabrics, however,

wetness increases the fabric weight  $w$ , and therefore the drag of a wet and fluttering fabric is expected to increase.

Considering that the product of  $w$  and  $G_n$  equals  $G$ , analysing the influence of  $w$  and  $G_n$  on  $C_D$  with a multiple regression, the equation of which is a sum (Eq. (19)) and not a product, seems to be a methodological mismatch. However, since  $w$  and  $G_n$  were expressed in logarithmic form, the equation  $\log(w) + \log(G_n) = \log(G)$  is a sum.

From the statistical data (Figs. 4 and 6), it seems that the  $G_{nP}$ -data provided slightly better correlations than the  $G_{nGT}$ -data, i.e., better  $R^2$ - and  $p$ -values. This result is not further surprising, since the flexural rigidity calculated from Pierce's method requires only one coordinate (Fig. 2), the bending length  $C$  ( $x=C, y=0$ ), obtained from  $L$  via Eq. (2), whereas the Grießer-Taylor method [14] requires a further coordinate, the intercept  $b$  of the straight fabric segment ( $x=0, y=b$ ), while the other coordinate of the endpoint of the overhanging fabric hinges on  $C$ :  $x=C$  and  $y=C \tan(-42.9^\circ)$ . The measurement of another coordinate introduces a source of error.

The limitations of this study are fourfold:

- (1) The fabric properties were restricted to  $w$  and  $G$ , and, e.g., air-permeability and fabric roughness were not included. Considering the three reasons for rejecting a multiple regression (as stated above), more than two predictors, e.g., three, increases the three equations, Eqs. (16–18), to seven [24], and the less likely it is that a multiple regression is justified. This problem is exemplified in Fig. 6, namely that for  $Re < 150$  k, multiple regressions are not applicable (except for  $Re = 90$  k).
- (2) Only eleven fabrics were tested in the wind tunnel. It was difficult to find an acceptable range of the combinations between stiff/soft and light/heavy. Particularly the combination of stiff and light was lacking. A similar problem arose in another study, requiring the combinations of grippy/slippy and smooth/rough surfaces, where the combination of rough and slippy was similarly difficult to find [25]. Nevertheless, eleven fabrics sufficed to provide the evidence that fluttering stiff and heavy fabrics have a larger  $C_D$ .
- (3) The dimensions of cylinder and fabric samples were based on the FIS rules as explained in the Methods section. The cylinder diameter should therefore be between that of a muscular thigh and upper arm and the looseness ratio should give a distance between the back surface of the cylinder and the rear edge of the pulled back fabric of 60 to 80 mm. Since the dimensions of body segments depend on body size, muscle thickness, body shape and gender differences, a one-size-fits-all cylinder is representative but evidently does not fit all dimensions. However, the aim of this study was to investigate the dependence of  $C_D$  on bending

stiffness and fabric weight on a cylinder size applicable to SX and SBX, but not on different body segment sizes on a larger scale.

- (4) To calculate the drag coefficient of the cylinder without and with fluttering fabrics, the frontal area was used in the present study. When considering the amplitude of the fluttering fabrics at the back of the cylinder, the change in area is inconstant and varies at a high frequency. Moreover, the frequent change in area cannot be measured accurately. A better approach would have been to express the aerodynamic parameter in terms of the drag area  $Ad (= C_D \cdot A)$  or in terms of the drag force  $F_D$ . However, for comparison purposes, especially with respect to the bare cylinder, it is more understandable to specify the  $C_D$  based on the frontal area of the cylinder, since the  $C_D$  of the subcritical cylinder is known to be about 1.1–1.25 [26].

The practical applicability of the results of this study, particularly for racing suits of ski and boardercross athletes, is seen as follows. That the  $C_D$  of lighter and more flexible fluttering fabrics is smaller than the  $C_D$  of the bare cylinder in the subcritical flow regime does not mean that we can expect the same results when applied to athletes' limb segments. This is due to the fact that limb segments are not necessarily aligned perpendicular to the free air-flow, and due to additional interference drag with the athlete's body. It is well known that fluttering fabrics generally do not work any better than a skinsuit. However, it is likely that lighter and more flexible fabrics will produce a drag force closer to that of a skin suit, as opposed to heavier and stiffer fabrics. The recommendation resulting from this study is that clothing for ski and boardercross athletes should be made of lighter and more flexible fabrics.

## 5 Conclusion

Both fabric weight  $w$  and flexural rigidity  $G$  increase the drag coefficient in fluttering garments. The flexural rigidity, normalised to the weight, appears to have a greater influence than weight itself. These principles should be taken into account when developing loose-fitting garments required in ski and boardercross.

## Appendix

Overview of the ski cross (SX) and snowboardcross (SBX) rules, related to the usage of clothing, issued by the International Ski and Snowboard Federation (FIS):

*Rule 6. Competition Suits / 6.1 Ski Cross (2022/2023 edition; [3]):*

*Suit base material shall be textile fabrics excluding rubber, neoprene, leather or vinyl like materials or fabrics. ... Material shall be uniform for the entire suit from top to bottom. ... Protection equipment including back protector or any other padding or body amour must be worn on the body and separate from the Ski Cross competition suit (outer wear). Protection and padding must not be built into the Ski Cross suit or attached to the Ski Cross suit by a zipper, velcro or any other means.*

Some years earlier, these rules were more detailed:

*Rule 6. Competition Suits / 6.1 Ski Cross (2018/2019 edition; [4]):*

*Suits worn in the Alpine events of Downhill (DH), Super-G (SG), Giant Slalom (GS), Slalom (SL) and Speed Skiing are not allowed. ... Fastening devices such as elastic straps, zippers, nylon straps, buttons, snaps, velcro, one or 2 sided tape, or any other methods shall not be used to tighten the pant leg material closer to the body or make the pant leg faired or aerodynamic.*

*The material gap shall be found everywhere at the measuring control points, without stretching or pulling the fabric apart from the underwear.*

*The measurement tool shall be certified by the FIS Office. Standardized measuring control points:*

*Lower Body: Anywhere below the person's mid point of the thigh to the bottom of the pant leg. The pant leg must cover the top of the skier's boot (top of ski boot is the area directly above the upper most buckle of the boot).*

*Upper Body: Mid-bicep (mid-bicep is found by finding the mid-point between the tip of one's elbow and the point on the top of the shoulder where the Acromion bone in the shoulder meets the head of the Humerus.)*

The rules in 2016/17 [5] went even further:

*Rule 6. Competition Suits / 6.1 Ski Cross (2016/17 edition; [5]):*

*The gap in the material must be a minimum of 80 mm, measured everywhere around the circumference of each leg from the mid-thigh to the top of the ski boot and 60 mm everywhere around the elbow and the bicep.*

The measurement tool referred to in the 2016/17 [5] and 2018/2019 [4] editions of the FIS rules is available from Settele Ltd. (Lindenberg, Germany) [6].

In snowboard cross (SBX), the International Ski and Snowboard Federation (FIS) has similar regulations [7]:

*Form fitting speed or downhill suites [sic] are not permitted. Non protruding body protection and padding is recommended. Protective equipment i.e. back protection must be worn on the body. No straps, fastening devices or other methods can be used to tighten the suit material closer to the body.*

These rules apply to the snowboard disciplines of SBX, slalom, and giant slalom.

Both SX rules (*Protection and padding must not be built into the Ski Cross suit or attached to the Ski Cross suit by a zipper, velcro or any other means [3]*) and the SBX rules (*No straps, fastening devices or other methods can be used to tighten the suit material closer to the body [7]*) imply that there must be a gap between the protectors (undergarment) and the competition suit (outer wear).

**Funding** Open Access funding enabled and organized by Projekt DEAL. This research did not receive any specific grant from funding agencies in the public, commercial, or not-for-profit sectors.

**Data Availability** The data presented in this study are available on request from the author to any qualified researcher.

## Declarations

**Conflict of interest** F. K. Fuss declares that he has no competing interests.

**Open Access** This article is licensed under a Creative Commons Attribution 4.0 International License, which permits use, sharing, adaptation, distribution and reproduction in any medium or format, as long as you give appropriate credit to the original author(s) and the source, provide a link to the Creative Commons licence, and indicate if changes were made. The images or other third party material in this article are included in the article's Creative Commons licence, unless indicated otherwise in a credit line to the material. If material is not included in the article's Creative Commons licence and your intended use is not permitted by statutory regulation or exceeds the permitted use, you will need to obtain permission directly from the copyright holder. To view a copy of this licence, visit <http://creativecommons.org/licenses/by/4.0/>.

## References

1. Brownlie LW (1992) Aerodynamic characteristics of sports apparel. PhD Thesis, Simon Fraser University, Burnaby, Canada
2. Chua JJC, Fuss FK, Troynikov O (2011) Aerodynamics of loose sports garments. *Proc Eng* 13:370–375. <https://doi.org/10.1016/j.proeng.2011.05.100>
3. FIS (2022/2023) Specifications for competition equipment; snowboard, freestyle, freeski and ski cross. Int Ski and Snowboard Federation (FIS): Oberhofen am Thunersee, Switzerland
4. FIS (2018/2019) Specifications for competition equipment, cross country/Ski Jumping/nordic combined, snowboard/freestyle/freeski. International Ski Federation (FIS): Oberhofen am Thunersee, Switzerland
5. FIS (2016/2017) Specifications for competition equipment and commercial markings. International Ski Federation (FIS): Oberhofen am Thunersee, Switzerland
6. Settele Ltd (nd) SX suit measurement tool: [https://settele-sport-systems.de/media/measurement\\_de.pdf](https://settele-sport-systems.de/media/measurement_de.pdf). Accessed April 20, 2024.
7. FIS (2017) The international snowboard competition rules (ICR), Book vi, joint regulations for snowboarding. International Ski Federation (FIS): Oberhofen am Thunersee, Switzerland
8. Oggiano L, Sætran L (2010) A low drag suit for ski-cross competitions. *Proc Eng* 2:2387–2392. <https://doi.org/10.1016/j.proeng.2010.04.004>

9. Carruthers AC, Filippone A (2005) Aerodynamic drag of streamers and flags. *J Aircraft* 42(4):976–982
10. Fairthorne RA (1930) Drag of Flags. Aeronautical Research Committee, Reports and Memoranda ARC/R&M-1345:887–91
11. Martin A (2006) Experimental study of drag from a fluttering flag. Master of Science Thesis, Oklahoma State University
12. ASTM (2020) ASTM D3776/D3776M-20, Standard Test Methods for Mass Per Unit Area (Weight) of Fabric. ASTM International, (American Society for Testing and Materials): West Conshohocken, PA, USA. [https://doi.org/10.1520/D3776\\_D3776M-20](https://doi.org/10.1520/D3776_D3776M-20)
13. ASTM (2023) ASTM D1388–18, Standard Test Method for Stiffness of Fabrics. ASTM International, (American Society for Testing and Materials): West Conshohocken, PA, USA. <https://doi.org/10.1520/D1388-18>
14. Griebner MT, Taylor EM (1996) The bending behaviour of fabrics: an energy approach. *Math Comp Simul* 41:579–586
15. Rudra RR, Mills JCT (1986) Flaw in the Shirley stiffness tester. *Textile Res J* 56:712. <https://doi.org/10.1177/004051758605601110>
16. Rao MVS, Talele AB, Mehta YC (1987) Comments on “Flaw in the Shirley Stiffness Tester.” *Textile Res J* 57:556. <https://doi.org/10.1177/004051758705700913>
17. Peirce, FT (1930) The ‘handle’ of cloth as a measurable quantity. *J Textile Inst* 21:T377–416, (T = J Textile Inst transactions)
18. Grosberg P (1966) The mechanical properties of woven fabrics, Part II: The bending of woven fabrics. *Textile Res J* 36:205–211
19. Fuss FK (2011) The effect of surface skewness on the super/postcritical coefficient of drag of roughened cylinders. *Proc Eng* 13:284–289. <https://doi.org/10.1016/j.proeng.2011.05.086>
20. Alam F, Steiner T, Chowdhury H, Moria H, Khan I, Aldawi F, Subic A (2011) A study of golf ball aerodynamic drag. *Proc Eng* 13:226–231. <https://doi.org/10.1016/j.proeng.2011.05.077>
21. James G, Witten D, Hastie T, Tibshirani R (2013) An introduction to statistical learning: with applications in R. Springer, New York NY, USA
22. Hoerner SF (1965) Fluid-dynamic drag. Hoerner Fluid Dynamics, Bakersfield CA, USA
23. Sudhakar Y, Vengadesan S (2012) Vortex shedding characteristics of a circular cylinder with an oscillating wake splitter plate. *Comput Fluids* 53:40–52
24. Fuss FK, Niegl G (2012) The importance of friction between hand and hold in rock climbing. *Sports Technol* 5(3–4):90–99. <https://doi.org/10.1080/19346182.2012.755539>
25. Fuss FK, Weizman Y, Niegl G, Tan AM (2020) Climbers’ perception of hold surface properties: roughness versus slip resistance. *Front Psychol*. <https://doi.org/10.3389/fpsyg.2020.00252>
26. Ma H, Duan Z (2020) Similarities of flow and heat transfer around a circular cylinder. *Symmetry*. <https://doi.org/10.3390/sym12040658>

**Publisher’s Note** Springer Nature remains neutral with regard to jurisdictional claims in published maps and institutional affiliations.